

The Effect of Periodic Friction and Upsetting Pressure on Rotary Friction Welding Process

Anmar Musaid Nayif * **Alaa Daham Younis ***
anmar.21enp87@student.uomosul.edu.iq alaayonis@uomosul.edu.iq
Ziad Shakeeb Alsarraf * **Muhsin M. Hamdoon ****
ziadalsarraf@uomosul.edu.iq muhsinaljubori@yahoo.com

* Mechanical Engineering Department, College of Engineering, University of Mosul, Mosul, Iraq

** Mechanical, Automotive, and Materials Engineering Department, University of Windsor, Windsor, Canada

Received: December 22th, 2024 Received in revised form: February 25th, 2024 Accepted: March 12th, 2024

ABSTRACT

This study investigates the impact of temperature and pressure on friction welding, a solid-state joining technique. It uses simulation to analyze material behavior and properties during the welding process. The study aims to optimize welding conditions to improve joint strength and integrity. The results provide recommendations for maximizing parameters in practical applications, enhancing production procedures and enhancing decision-making. The simulation-based methodology also offers an economical and expedient method for investigating situations before experimental execution. The test rod, measuring 16mm in diameter and 100mm in length, was designed for two pieces. The simulation program was set up with timings and pressures, a fixed rotation speed of 1500 r.p.m., and the temperatures from the welding process were entered into an artificial intelligence SIMULIK program. The study reveals that the deformations of the materials being welded are directly influenced by the welding pressure. Greater force is given to the materials as pressure rises, which causes more plastic deformation. and longer times under frictional pressure can lead to higher temperatures due to increased heat generation from friction. This enhanced metallurgical bonding can result in a joint with improved fatigue strength. which can contribute to better fatigue resistance. Prolonged welding pressure helps in reducing stress concentrations at the weld interface. and the stress distribution will be more uniform, minimizing the likelihood of stress concentration points in the weld joints with fewer defects and improving resistance to crack initiation and propagation.

Keywords:

Fatigue, number of cycles to failure, Artificial neural network (ANN), Upsetting pressure, Heating pressure.

This is an open access article under the CC BY 4.0 license (<http://creativecommons.org/licenses/by/4.0/>).

<https://rengj.mosuljournals.com>

Email: alrafidain_engjournal2@uomosul.edu.iq

1. INTRODUCTION

This study aims to improve our understanding of how changes in heating time and upsetting pressure affect friction welding. It focuses on adjusting heating duration and upsetting pressure during the simulation of friction welding. The goal is to find the ideal combination of heating time and upsetting pressure for better joint characteristics. The results could improve friction welding procedures, leading to increase welding efficiency, dependability, and joint strength. Simulation tools can offer insights into the impacts of parameters changes, thereby reducing equipment and material costs. In this

study, ANN was trained by inputting temperatures and S-N curve values and obtaining new S-N values for other cases.

[1] Salih et. al (2022) simulated the RFW process, and mathematical models and compared them with the experimental results obtained from previous research, which showed that a rise in temperature leads to a change in mechanical properties. The heat generated into heat generated by rotating and sliding friction and is generated during plastic deformation. With the temperature rising, the yield stress reduces until it becomes less than the flow stress, and then the plastic deformation starts. [2] Ullegaddi, Balappa,

and Babu (2023) used finite element analysis by Ansys Workbench to simulate mechanical and thermal impacts simultaneously. And obtained elevated temperatures concerning time from the transient thermal analysis. Therefore, the model developed in this study can be used to simulate the friction welding process. [3] Nam, Trung, and Khanh (2024) presented a study on the effect of the annealing solution process on RFW joints of Al 6061 and selected the optimal parameters for the process. They evaluated the quality of welded joints through a series of experiments measuring hardness, and tensile strength tests. [4] Mercan, Aydin, and Özdemir (2015) used RFW process to connect AISI 2205 and AISI 1020 using different parameters. Tensile tests and rotational bending fatigue tests were conducted on welded joints to study the effects of welding parameters on fatigue strength. It was found that the fatigue strength of the connection increased compared to the primary material. [5] In their study, Sasmito, Suhartono, and Sunyoto (2024) presented experimental results of RFW of AA5083-H112 and AA7075-T6 at four-time intervals and a constant rotational speed of 1700 r.p.m. focused on studying the effect of welding parameters on joint performance and evaluating it through mechanical testing, metallographic, and hardness testing. The effect of temperature on joint toughness was evaluated through Charpy impact tests at different temperatures. [6] In Mortazavi and Ince's (2020) study, a radial basis function model has been developed to predict the fatigue crack initiation behavior. The presented ANN model was trained and verified by experimental data of titanium alloy Ti-6Al-4V, 2024-T3, and aluminum alloy 7075-T6. The results showed that ANN model has a good capability to predict the nonlinearity of crack initiation behavior.

According to the reviewed work, it can be concluded that most of the studies seem to focus on specific materials, such as stainless steel and carbon steel. While finite element methods are commonly used, exploring, and developing more advanced simulation techniques could enhance the accuracy and efficiency of predicting friction welding outcomes.

This work explores the use of rotary friction welding to fuse aluminum alloys AA7075 and AA5083 which are different. Temperature inputs are incorporated into an artificial neural network (ANN) to forecast S-N curve values for fatigue analysis. The ANN's ability to anticipate and compare welding outcomes is demonstrated by comparing results across different materials.

2. MATERIALS

The AA5083 and AA7075 aluminum alloys rods that were employed in this investigation were treated with H112 and T6, respectively.

2.1 AA5083 H112 Aluminum alloy

This alloy has moderate strength and extremely strong corrosion resistance (albeit it can deteriorate with extended exposure to high temperatures). And that it can be welded. It is used in gas/oil pipes, drilling rigs, towers, pressure vessels, transportation, ordnance, and armor plates table 1 and Table 2 shows chemical composition Mechanical properties respetively [7].

Table 1. chemical composition of the Aluminum alloy AA5083 H112 [7]

Components	Per %
Aluminum (Al)	92.4 - 95.6
Chromium (Cr)	0.05 - 0.25
Copper (Cu)	0.10
Iron (Fe)	0.40
Magnesium (Mg)	4.0 - 4.9
Manganese (Mn)	0.40 - 1.0
Other (each)	0.05
Other (total)	0.15
Silicon (Si)	0.40
Titanium (Ti)	0.15
Zinc (Zn)	0.25

Table 2. Mechanical properties of the Aluminum alloy AA5083 H112 [7]

Mechanical Property	
Hardness (Brinell)	81
Hardness (Knoop)	104
Hardness (Rockwell B)	50
Hardness (Vickers)	91
Tensile Strength (Ultimate)	294.6 ± 5.4 Mpa
Tensile Strength (Yield)	176.6 ± 14.9 MPa
Modulus of Elasticity	70.30 Gpa
Compressive Modulus	71.70 Gpa
Poissons Ratio	0.33
Shear Modulus	26.40 Gpa
Shear Strength	Mpa

2.2 AA7075 T6 Aluminum alloy

7075 is Part of the 7000 Series of aluminum alloys, which is regarded as the strongest aluminum alloy series for use in aircraft applications. Its high strength, toughness, strong fatigue resistance, good ductility, and outstanding mechanical qualities are all present table 3 and table 4 shows chemical composition Mechanical properties respetively .[8]

Table 3. chemical composition of the Aluminum alloy AA7075 T6 [9]

Components	Per %
Aluminum (Al)	87.1 - 91.4 %
Chromium (Cr)	0.18 - 0.28 %
Copper (Cu)	1.2 - 2.0 %
Iron (Fe)	0.50 %
Magnesium (Mg)	2.1 - 2.9 %
Manganese (Mn)	0.30 %
Other (each)	0.05 %
Other (total)	0.15 %
Silicon (Si)	0.40 %
Titanium (Ti)	0.20 %
Zinc (Zn)	5.1 - 6.1 %

Table 4. Mechanical properties of the Aluminum alloy AA7075 T6 [9]

Mechanical Property	
Hardness (Brinell)	150
Hardness (Knoop)	191
Hardness (Rockwell B)	87
Hardness (Vickers)	175
Tensile Strength (Ultimate)	592.6 ± 7.7 Mpa
Tensile Strength (Yield)	414.8 ± 5.3 Mpa
Modulus of Elasticity	71.7 GPa
Poissons Ratio	0.33
Machinability	70 %
Shear Modulus	26.9 GPa
Shear Strength	331 MPa

3. THE ROTARY FRICTION WELDING PROCESS

In this project, the samples were created in the shape of a 100 mm long, 16 mm diameter cylindrical rod, the second rod, AA7075, served as the rotating side (RS), and the cylindrical rod AA5083 was positioned as the stationary side (SS) that was moved axially. The moving surface contacted the stationary surface. The welding process's first step involved a rapid increase in axial Heating pressures 30, 40, and 50 Mpa. then involved friction at constant Upsetting pressures 60, 70, and 80 MPa. The production of bonds was triggered by the interruption of the rotational speed at the end of the friction stage and the application the upset pressure [10].

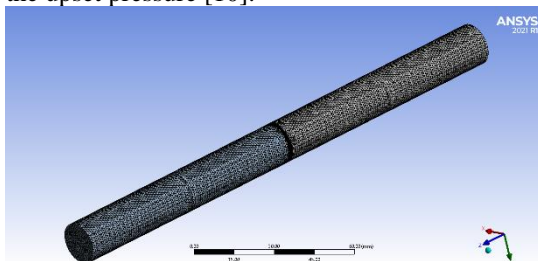


Figure 1: Mesh generated.

The simulation process depends on complicated algorithms to solve the matrices present in the domain so, an accurate mesh created to solve the equations. The mesh used was a fine tetrahedron with number of elements 347455 when the max temperature reached 691.8 C.

Table (5): Mesh independency

case	element	node	Max temperature C
1	195364	235467	702.8
2	262456	305678	693.5
3	305685	416764	691.9
4	347455	501473	691.8

The simulation program settings were made with timings and pressures as in Table 6, with a fixed rotation speed that does not change with changing tests, and its value is 1500 r.p.m.

Table (6): Layout of experimental parameters using an orthogonal array [10].

no.	Heating Pressure	Time	Upsetting pressure	time
1	30 (MPa)	3 (sec)	60 (MPa)	2 (sec)
2	30 (MPa)	4 (sec)	70 (MPa)	3 (sec)
3	30 (MPa)	5 (sec)	80 (MPa)	4 (sec)
4	40 (MPa)	3 (sec)	70 (MPa)	4 (sec)
5	40 (MPa)	4 (sec)	80 (MPa)	2 (sec)
6	40 (MPa)	5 (sec)	60 (MPa)	3 (sec)
7	50 (MPa)	3 (sec)	80 (MPa)	3 (sec)
8	50 (MPa)	4 (sec)	60 (MPa)	4 (sec)
9	50 (MPa)	5 (sec)	70 (MPa)	2. (sec)

4. ARTIFICIAL NEURAL NETWORK [ANN]

The extracted temperatures from the simulation of the welding process were entered into the artificial intelligence program to obtain the values of the S-N curve. As depicted in Figure 2, the Artificial Neural Network (ANN) technique requires training a machine learning model to forecast the fatigue life of a material under cyclic loading circumstances in order to predict an SN (Stress-Life) curve, which is an important tool in analyzing structures and materials science. The fatigue database should include the stress level (S) and the number of cycles to failure (N) for various specimens or materials. These parameters are necessary for validating and training ANN models. All input features (stress levels) and output features (cycles to failure) should be normalized to ensure they have equivalent scales that facilitate faster convergence of the neural network during training[14].

5. FATIGUE CRACKS

The fatigue simulation model was designed according to the dimensions mentioned in Figure 3. This sample resulted from the simulation of rotary friction welding, where the

length of the sample was 90 mm and its diameter was 12 mm.

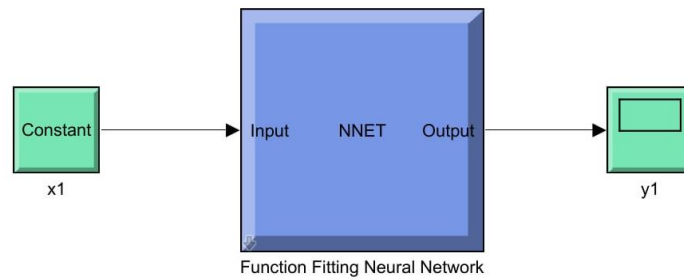


Figure 2: ANN diagram

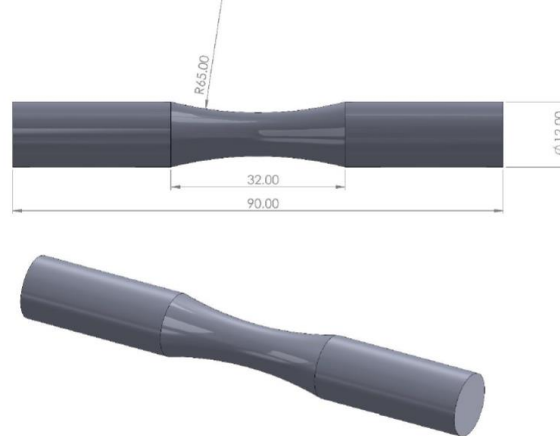


Figure 3: Fatigue Cracks domain

Where the process of stabilizing the sample was carried out on the one hand, and a pressure was used to obtain the fatigue state in the sample during the simulation process.

The fatigue analysis in ANSYS Workbench estimates the number of cycles to failure using a variety of fatigue life estimation techniques, including the Stress-Life (S-N) and Strain-Life (-N) approaches. The specific material qualities, loading conditions, and method selected all affect the equations that are utilized for fatigue analysis. The equation used to calculate the fatigue life (N) for a Stress-Life (S-N) approach in ANSYS, which is frequently utilized for metals, is frequently represented as [11]:

$$N = (A/(\sigma)^m) + (B/(\sigma)^n) \quad (1)$$

Where: The cycle count before failure is N. The amplitude of the alternating stress is σ .

Material specific constants A, B, m, and n are identified by data from fatigue tests or by material characteristics. Similar equations are utilized in the Strain-Life (-N) approach, which is used for materials that display strain-based fatigue behavior, although the terms and constants may be connected to strain rather than stress.

6. RESULTS AND DISCUSSION

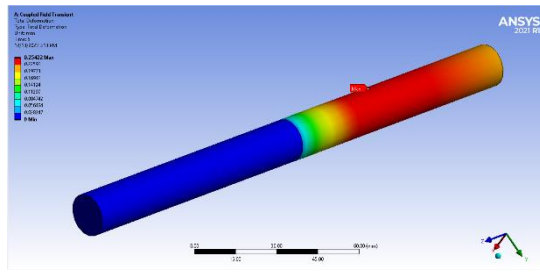
In this paragraph, all the cases and tests that were studied will be included for comparison among themselves and the effect of the duration of friction and welding pressures that were studied.

6.1 Effect of upsetting pressure

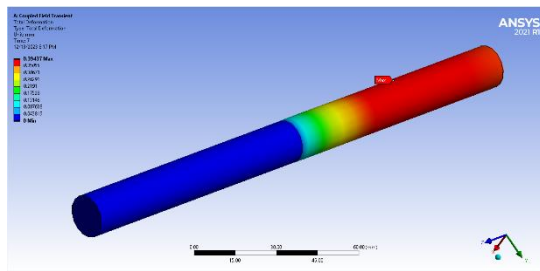
Friction welding is a solid-state welding technique that uses mechanical friction between two workpieces to produce heat. The process involves touch and friction, followed by a phase of upsetting (pressure) where axial pressure is applied to force materials together. Upsetting pressure significantly impacts the final weld's strength and quality, facilitating material bonding, reducing the possibility of flaws, ensuring joint strength, and fine-tuning the grain structure. It can also be used to manage the welding process by varying the upsetting pressure. The ideal upsetting pressure depends on the materials, characteristics, and finished product demands.

In Figures 4 and 5, which represents the deformations resulting from the friction welding process, it is noted that the value of the deformations increases with increasing welding pressure, as it was at a welding pressure of 60 MPa and reached 0.254 mm, while at a welding pressure of 70 MPa it reached 0.394 mm. As for the last

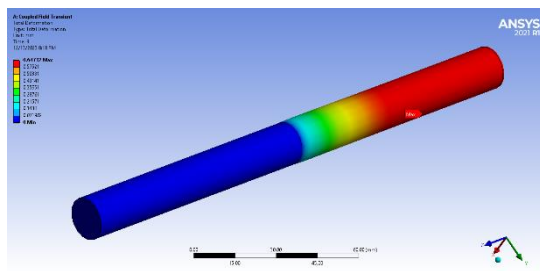
pressure state represented by the welding pressure 80 MPa, it reached 0.647 mm.



(a)



(b)



(c)

Figure 4: Deformation contour of 30 MPa friction pressure at different Upsetting pressure. (a) 60 MPa, (b) 70 MPa, (c) 80 MPa.

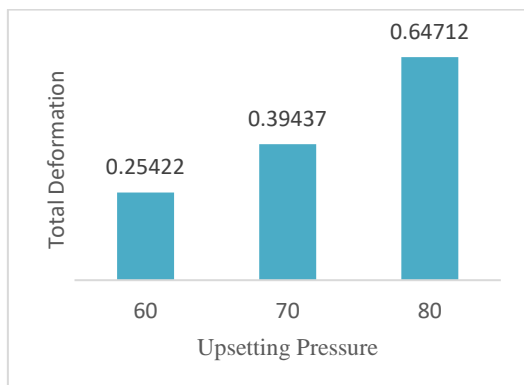
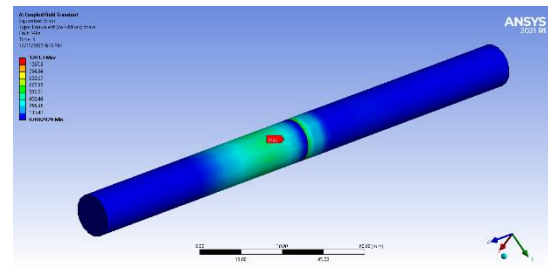


Figure 5: Deformation of 30 MPa friction pressure at different Upsetting pressure.

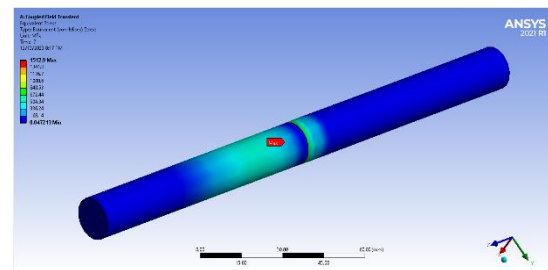
Plastic Flow and distortion are responsible for the rise in distortion with increased welding pressure. The plastic flow and distortion

of the materials being welded are directly influenced by the welding pressure. Greater force is given to the materials as pressure rises, which causes more plastic deformation. Additionally, a greater contact area between the two materials is produced by higher welding pressure. and the softening of the materials at the welding contact may be the consequence of both frictional heating and elevated pressure. The materials are more prone to plastic deformation when they have softened. [12]

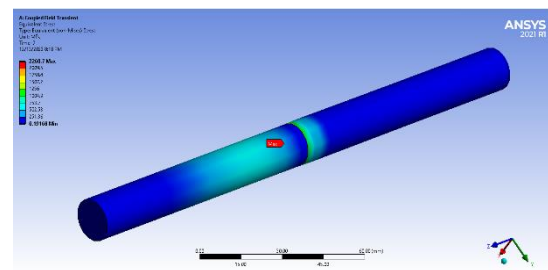
In figures 6 and 7 illustrates the stress resulting from the friction welding process. As the welding pressure increases, the stress value increases as well. The stress peaked at 1201 MPa at 60 MPa and at 1512 MPa at 70 MPa. The welding pressure of 80 MPa indicated that it had reached the final pressure condition of 2260 MPa.



(a)



(b)



(c)

Figure 6: Equivalent Stress contour of 30 MPa friction pressure at different welding pressure. (a) 60 MPa, (b) 70 MPa, (c) 80 MPa.

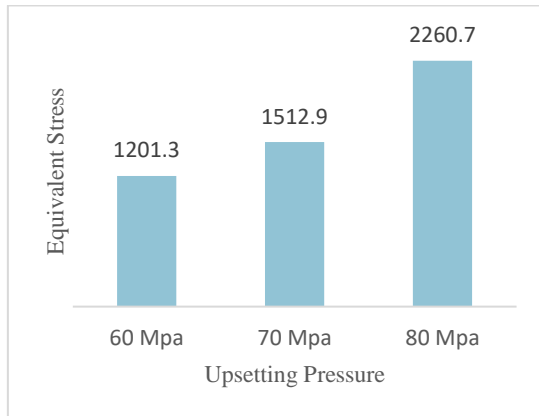
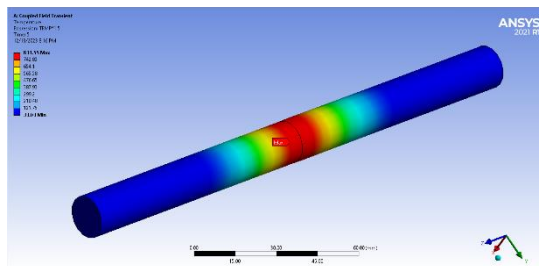


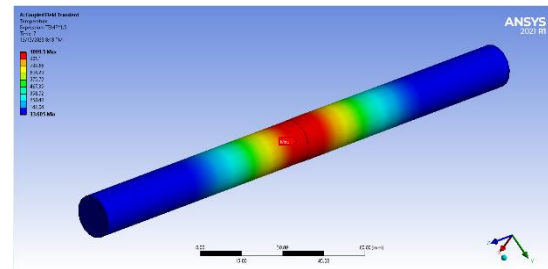
Figure 7: Equivalent Stress of 30 MPa friction pressure at different welding pressure.

The increase in equivalent stress with increasing welding pressure can be attributed to the applied Forces Increasing welding pressure directly increases the forces applied to the materials during the welding process. This elevated pressure results in higher stress being exerted on the materials at the welding interface. Aluminum alloys, including AA5083 and AA7075, undergo plastic deformation when subjected to stress. Higher welding pressure increases the plasticity of the materials, causing them to deform more readily and thus experience higher equivalent stress.

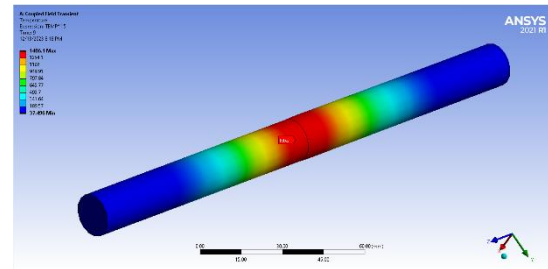
Figures 8 and 9, which depicts the temperature arising from the friction welding process, shows that the value of the temperature increases with increasing welding pressure, as it was at 60 MPa and reached 831 C, while at 70 MPa it reached 1009 C. The final pressure state, indicated by the welding pressure of 80 MPa, reached 1409 C.



(a)



(b)



(c)

Figure 8: Temperature contour of 30 MPa friction pressure at different welding pressure. (a) 60 MPa, (b) 70 MPa, (c) 80 MPa.

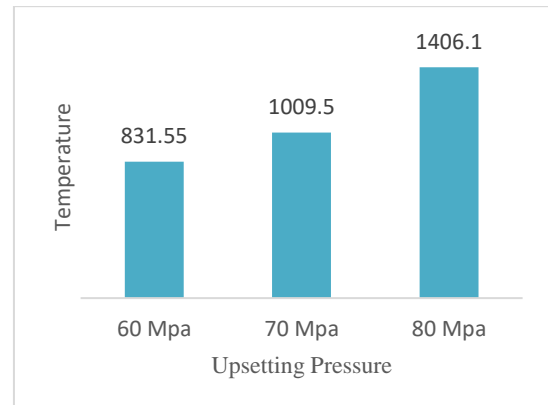


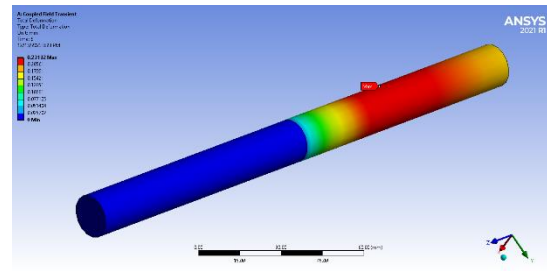
Figure 9: Temperature of 30 MPa friction pressure at different welding pressure.

When higher pressure is applied during rotary friction welding Higher pressure enhances the contact between the materials being welded, increasing the frictional force between them. This increased friction results in greater heat generation at the interface. The higher pressure can also lead to better material deformation, aiding in the creation of a more uniform and thorough bond between the materials. Increased pressure can contribute to better intermolecular mixing of the materials at the weld interface, promoting the formation of a strong metallurgical bond.

6.2 Effect of heating pressure

Friction welding involves the use of mechanical friction between two surfaces to heat up the weld. The success of the weld depends on the heating pressure, also known as axial pressure, during the heating phase. This pressure influences temperature generation, material softening, microstructure evolution, material flow and bonding, and overall weld quality. Control over the heating pressure is crucial to avoid overheating and material ejection. Proper management of heating pressure can optimize the process, minimizing faults and achieving required weld qualities. The precise parameters, including heating pressure, may change based on the materials being welded, the application, and the materials themselves.

In Figures 10 and 11, with changing the heat pressure value, it is noted that an increase in the heat pressure time increases the deformation value, as it reached 0.647 mm at a heat pressure of 30 and a time of 5 seconds. The deformation occurring in the metal piece during the simulation is based on one principle, which is the movement of the element from one point to another, whether the cause is rotation or movement of the metal rod or the result of stress and strain in the piece, as the deformation is not limited only to the process of interference in welding but rather to the speed of rotation of the facing piece. for welding process



(c)

Figure 10: Deformation contour of 80 MPa welding pressure at different friction pressure. (a) 30 MPa and time 5 s, (b) 40 MPa and time 4 s, (c) 50 MPa and time 3 s.

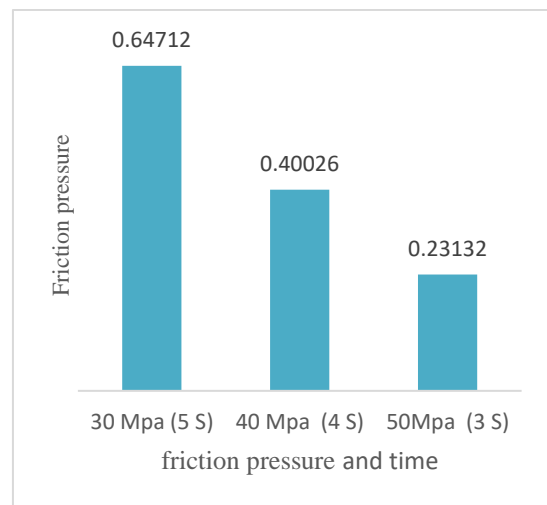
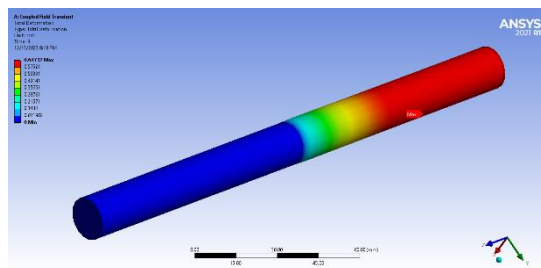
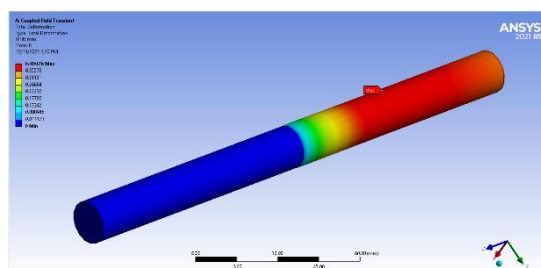


Figure 11: Deformation contour of 80 MPa welding pressure at different friction pressure and time



(a)



(b)

The additional time under frictional pressure promotes metallurgical bonding between the materials. This is essential for creating a strong, durable weld. Longer times under frictional pressure can lead to higher temperatures due to increased heat generation from friction. The elevated temperature contributes to the plasticity of the materials, allowing for more significant deformation. While increased deformation can be desirable for achieving a robust weld, it's important to balance this with other factors. and excessive deformation may lead to material flow issues, distortions, or other undesired effects. Therefore, the time of friction pressure needs to be carefully controlled and optimized based on the specific materials, geometry, and quality requirements of the welding application.

Figures 12 and 13, illustrates how altering the heat pressure value causes the stress value to increase as the heat pressure time does. At a heat pressure of 30 and a time of 5 seconds, the stress value reached 2260 MPa.

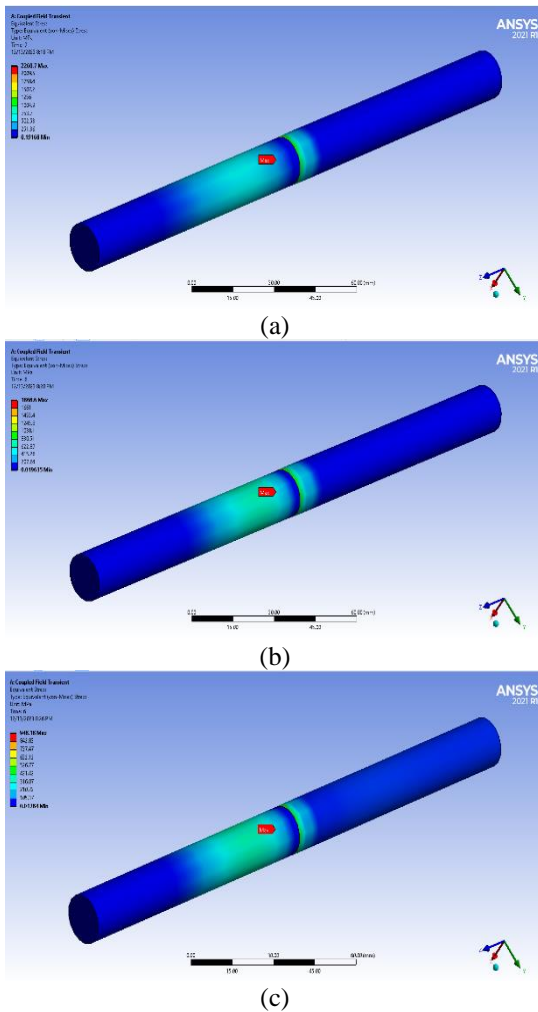


Figure 12: Stress contour of 80 MPa welding pressure at different friction pressure. (a) 30 Mpa and time 5 s, (b) 40 MPa and time 4 s, (c) 50 MPa and time 3 s.

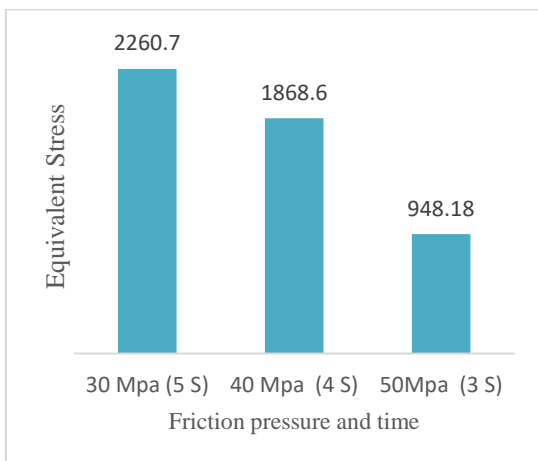


Figure 13: Equivalent Stress of 80 MPa welding pressure at different friction pressure and time.

Longer friction pressure times allow for more plastic deformation of the materials. This

increased deformation may contribute to higher equivalent stresses, especially in areas where the material is undergoing significant changes in shape. and leads to higher temperatures. Elevated temperatures can soften the material, making it more susceptible to plastic deformation and altering the distribution of stresses.

Figures 14 and 15, shows that increasing the heat pressure duration raises the temperature value, as it reached 1406 C at a heat pressure of 30 and a time of 5 seconds.

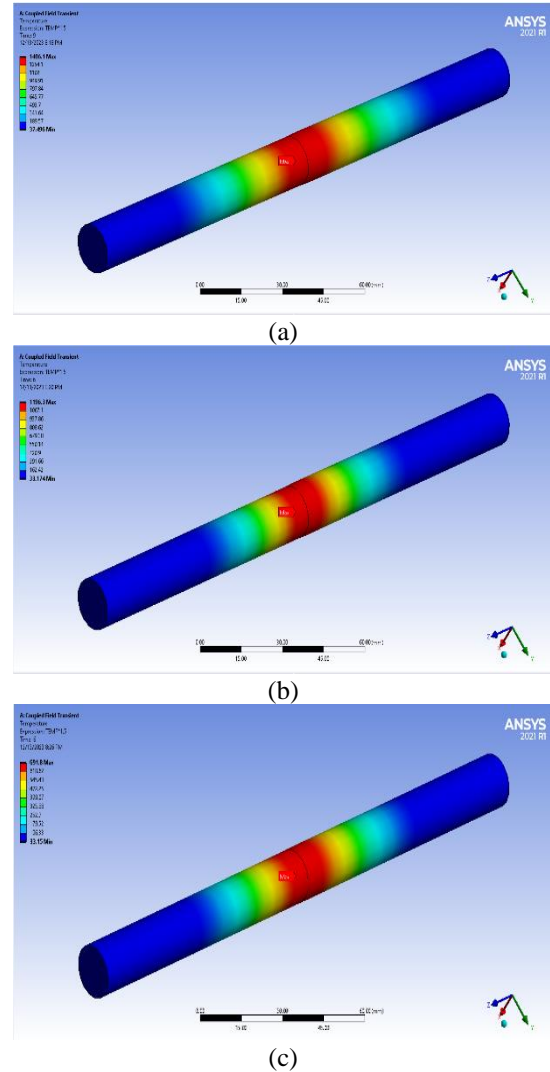


Figure 14: Temperature contour of 80 MPa welding pressure at different friction pressure. (a) 30 MPa and time 5 s, (b) 40 MPa and time 4 s, (c) 50 MPa and time 3 s.

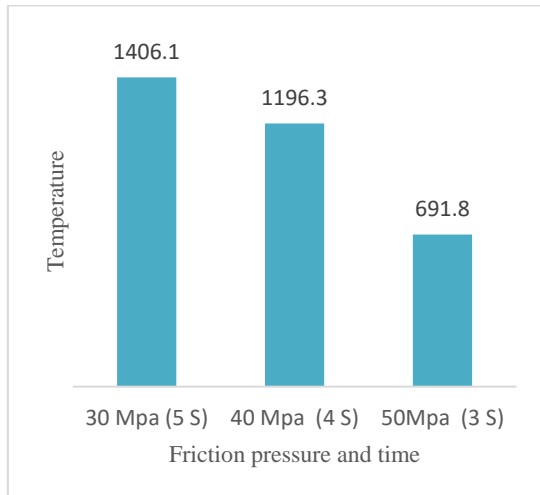
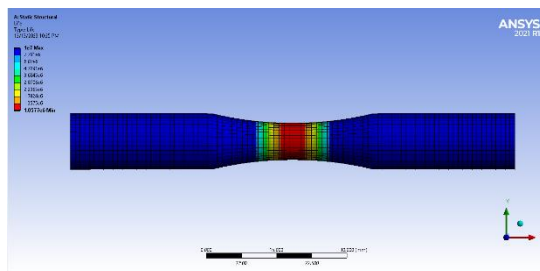


Figure 15: Temperature of 80 MPa welding pressure at different friction pressure and time

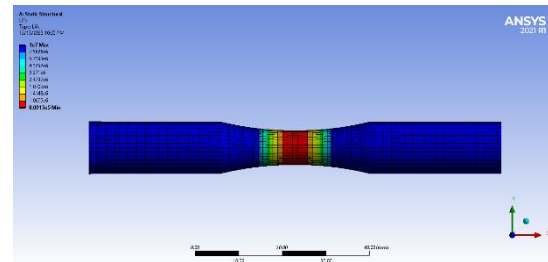
The increase in heat when increasing the time of friction pressure in rotary friction welding is related to the extended duration of the frictional forces acting on the materials. While increasing the friction pressure itself does contribute to heat generation, increasing the time allows for more sustained frictional contact, resulting in a greater overall accumulation of heat. The primary source of heat in rotary friction welding is the conversion of mechanical energy into thermal energy during friction. When you increase the time of friction pressure, the materials are in contact for a longer duration, allowing more time for the conversion of mechanical energy to heat. and then plastic deformation and improved bonding between the materials.

7. FATIGUE LIFE

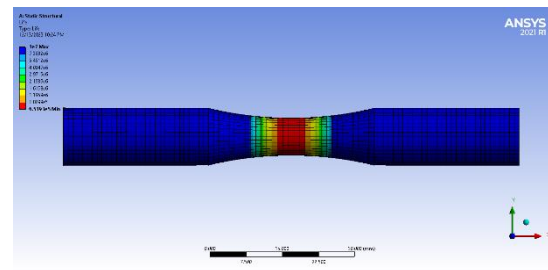
From Figures 16 and 17, increasing the rotation time increases the life resulting from the friction pressure, as the minimum life reached 651,930 cycles at the friction pressure of 50 MPa, and at the friction pressure of 40 MPa, the minimum life reached 809,150 cycles, while at the welding pressure 30 MPa. The minimum lifetime reached 1,057,700 cycles.



(a)



(b)



(c)

Figure (16): Life contour of 80 MPa welding pressure at different friction pressure. (a) 30 MPa and time 5 s, (b) 40 MPa and time 4 s, (c) 50 MPa and time 3 s.

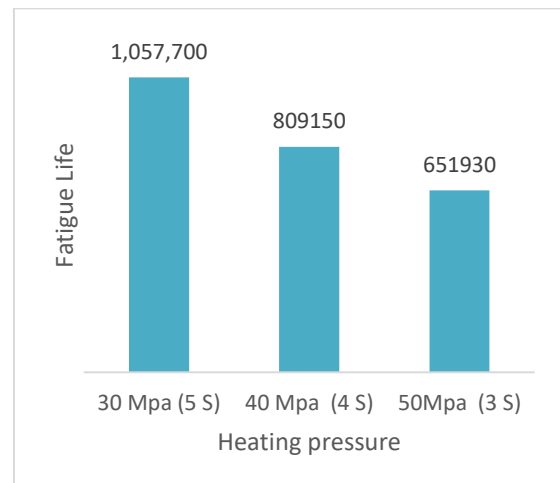


Figure (17): Fatigue life of 80 MPa welding pressure at different friction pressure and time.

Increasing time of applying the welding pressure allows for a more thorough bonding between the materials being welded. This enhanced metallurgical bonding can result in a joint with improved fatigue strength. and provides to achieve proper plastic deformation and create a strong, durable bond, which can contribute to better fatigue resistance. Prolonged welding pressure helps in reducing stress concentrations at the weld interface. and the stress distribution will be more uniform, minimizing the likelihood of stress concentration points in the weld joints with fewer defects and improving resistance to crack initiation and propagation.

8. CONCLUSION AND RECOMANDATIONS

8.1 Conclusion

1. Plastic flow and distortion are the reasons for the rise in distortion that occurs when welding pressure increases. The plastic flow and distortion of the materials being welded are affected by the welding pressure. More force is exerted to the materials at higher pressure, which causes more plastic deformation.
2. Increased welding pressure makes the materials more malleable, which makes them more prone to deformation and greater equivalent stress.
3. Because friction generates more heat over longer periods of time, temperatures can rise because of frictional pressure. The materials' increased flexibility as a result of the higher temperature permits more substantial deformation.
4. The longer duration of the frictional forces acting on the materials is connected to the rise in heat that occurs when the friction pressure is increased during rotary friction welding. While raising the friction pressure directly causes heat to be generated, doing so for a longer period of time permits more continuous frictional contact, which increases the amount of heat that is accumulated overall.
5. An even stronger connection between the materials being welded is possible when the welding pressure is applied for longer periods of time. By achieving appropriate plastic deformation and forming a strong, long-lasting connection, this improved metallurgical bonding can provide a joint with increased fatigue strength as well as resistance to fracture initiation and propagation.

8.2 Recomendations

Examining other options for rotary friction welding optimization and various combinations of welding pressure, friction pressure, and rotating speed affects the quality of joints. to encompass a wider variety of composite materials or alloys in the research. Expanding the use of ANN beyond rotary friction welding to investigate fatigue behavior in different welding processes.

REFERENCES

- [1] F. I. Salih, A. S. Dawood, and A. A. Hamid, "Review on the Thermal Characterizations of Rotary Friction Welding," *Al-Rafidain Engineering Journal (AREJ)*, vol. 27, no. 1, pp. 110–115, Mar. 2022, doi: 10.33899/rengj.2021.132049.1141.
- [2] M. Ullegaddi, B. Balappa, and N. Babu, "Finite Element Analysis of Rotary Friction Welding Process," 2023.
- [3] P. Nam, P. Trung, and B. Khanh, "A Study on Optimizing the Parameters of the Heat Treatment Process on Rotary Friction Welding of Aluminum Alloy A6061," *Key Engineering Materials*, vol. 975, pp. 71–77, Feb. 2024, doi: 10.4028/p-o0LhWr.
- [4] S. Mercan, S. Aydin, and N. Özdemir, "Effect of welding parameters on the fatigue properties of dissimilar AISI 2205–AISI 1020 joined by friction welding," *International Journal of Fatigue*, vol. 81, pp. 78–90, Dec. 2015, doi: 10.1016/j.ijfatigue.2015.07.023.
- [5] A. Sasmito, H. A. Suhartono, and Sunyoto, "Rotary friction welding properties of AA5083-H112/AA7075-T6 joints: Parameter and low temperature effect," *Materials Science and Technology*, vol. 40, no. 12, pp. 941–949, Mar. 2024. doi:10.1177/02670836241234198.
- [6] S. N. S. Mortazavi and A. Ince, "An artificial neural network modeling approach for short and long fatigue crack propagation," *Computational Materials Science*, vol. 185, p. 109962, Dec. 2020, doi: 10.1016/j.commatsci.2020.109962.
- [7] "Aluminum 5083-H112." Accessed: Dec. 14, 2023. [Online]. Available: <https://www.matweb.com/search/DataSheet.aspx?MatGUID=bd6317b19dd94faf8bff851e4f339e88&ckck=1>
- [8] "aa7075 T6 - Google Search." Accessed: Dec. 14, 2023. [Online]. Available: https://www.google.com/search?q=aa7075+T6&sca_esv=590835004&bih=674&biw=1511&rlz=1C1GCEB_enIQ1030IQ1030&hl=en&ei=cs96ZYOVh8aoxc8Pv6-esAI&ved=0ahUKEwiDsJT_0o6DAxVGVPEdHb-XByYQ4dUDCBA&uact=5&oq=aa7075+T6&gs_lp=Egxn3Mtd2l6LXNlcnAiCWFhNzA3NSBUNjIIFEAAYgAQyBRAAGIAEMgsQABiABBiKBRiGAzILEAAyAQYigUYhgMyCxAAAGIAEGIoFGIYDSNYVUMQKWKINcAF4AZABAJgB8AGgAdEDqgEDMi0yuAEDyAEA-AEBwgIKEAAYRjxjWBBiwA8ICBhAAGBYYHuIDBBgAIEGIBgGQBgg&scIent=gws-wiz-serp
- [9] M. Kerster, "Alloy Comparison: 7075-T6 Aluminum VS 7075-T62 Aluminum," AAA Air Support. Accessed: Dec. 14, 2023. [Online]. Available: <https://www.aaaairsupport.com/alloy-comparison-7075-t6-aluminum-vs-7075-t62-aluminum/>
- [10] M. Asif, M. K. A. Shrikrishana, and P. Sathiya, "Finite element modelling and characterization of friction welding on UNS S31803 duplex stainless steel joints," *Engineering Science and Technology, an International Journal*, vol. 18, no. 4, pp. 704–712, Dec. 2015. doi:10.1016/j.jestch.2015.05.002.
- [11] "Ansys | Engineering Simulation Software.' www.ansys.com, ansys.com," [Online]. Available: https://www.google.com/search?q=%E2%80%99CAnsys+%7C+Engineering+Simulation+Software.%E2%80%9D+Www.ansys.com%2C+ansys.com.&oq=%E2%80%99CAnsys+%7C+Engineering+Simulation+Software.%E2%80%9D+Www.ansys.com%2C+ansys.com.&gs_lcrp=EgZjaHJV

bWUyBggAEEUYOdIBCDEwMjJqMGo3qAIA
sAIA&sourceid=chrome&ie=UTF-8
[12] "Aluminium Alloys - Aluminium 5083
Properties, Fabrication and Applications,"

AZoM.com. Accessed: Oct. 26, 2023. [Online].
Available:https://www.azom.com/article.aspx?Art
icleID=2804

تأثير مدة الاحتكاك والضغط المسلط على عملية اللحام بالاحتكاك الدوار

علاء دحام يونس*
alaayonis@uomosul.edu.iq

انمار مساعد نايف*
anmar.21enp87@student.uomosul.edu.iq

محسن محمود حمدون*
muhsinaljubori@yahoo.com

زياد شكيب الصراف*
ziadalsarraf@uomosul.edu.iq

* قسم الهندسة الميكانيكية، كلية الهندسة، جامعة الموصل، موصل، العراق
** قسم الهندسة الميكانيكية والسيارات وهندسة المواد، كلية الهندسة، جامعة وندسور، وندسور، كندا

تاريخ القبول: 12 مارس 2024

استلم بصيغته المنقحة: 25 فبراير 2024

تاريخ الاستلام: 24 ديسمبر 2023

الملخص

تبحث هذه الدراسة في تأثير درجة الحرارة والضغط على اللحام الاحتكاكي، وهي تقنية ربط الحالة الصلبة. ويستخدم المحاكاة لتحليل سلوك المواد وخصائصها أثناء عملية اللحام. تهدف الدراسة إلى تحسين ظروف اللحام لتحسين قوة المفاصل وسلامتها. تقدم النتائج توصيات لتعظيم المعلمات في التطبيقات العملية، وتعزيز إجراءات الإنتاج وتعزيز عملية صنع القرار. كما توفر المنهجية القائمة على المحاكاة طريقة اقتصادية ومفيدة للتحقيق في المواقف قبل التنفيذ التجريبي. تم تصميم قضيب الاختبار، الذي يبلغ قطره 16 ملم وطوله 100 ملم، لقطعتين. وتم إعداد برنامج المحاكاة بالتوقيينات والضغط وسرعة دوران ثابتة تبلغ 1500 دورة في الدقيقة، كما تم إدخال درجات الحرارة الناتجة عن عملية اللحام إلى برنامج الذكاء الاصطناعي. كشفت الدراسة أن تشوهات المواد التي يتم لحامها تتأثر بشكل مباشر بضغط اللحام. يتم إعطاء قوة أكبر للمواد مع ارتفاع الضغط، مما يسبب المزيد من تشوه البلاستيك. ويمكن أن تؤدي الأوقات الأطول تحت ضغط الاحتكاك إلى ارتفاع درجات الحرارة بسبب زيادة توليد الحرارة من الاحتكاك. يمكن أن يؤدي هذا الترابط المعدني المعزز إلى تحسين قوة المفصل. والتي يمكن أن تساهم في تحسين مقاومة التعب. يساعد ضغط اللحام المطول في تقليل تركيزات الضغط في واجهة اللحام. وسيكون توزيع الإجهاد أكثر اتساقاً، مما يقلل من احتمالية وجود نقاط تركيز الإجهاد في وصلات اللحام مع عدد أقل من العيوب وتحسين المقاومة لبدء الشقوق وانتشارها.

الكلمات الدالة :

الكلال، عدد الدورات حتى الفشل، الشبكة العصبية الاصطناعية (ANN)، ضغط اللحام، ضغط التسخين.